Lattice-Boltzmann model based on field mediators for immiscible fluids

L. O. E. Santos,[1,*] P. C. Facin,[2,†] and P. C. Philippi[1,‡]
[1]*Mechanical Engineering Department, Federal University of Santa Catarina, 88040-900 Florianópolis, Santa Catarina, Brazil*
[2]*Physics Department, State University of Ponta Grossa, 84030-900 Ponta Grossa, Paraná, Brazil*
(Received 19 December 2002; revised manuscript received 19 August 2003; published 7 November 2003)

In this paper, a lattice BGK (Bhatnagar-Gross-Krook) model is proposed for immiscible fluids. Collision operator is decoupled considering mutual and cross collisions between lattice particles, with three independent parameters related to the species diffusivity and to the viscosity of each fluid. Field mediator's concept, described by Santos and Philippi [Phys. Rev. E **65**, 046305 (2002)], is extended to the framework of the lattice-Boltzmann equation and interference between mediators and particles is modeled by considering that there is a deviation in particles velocity, proportional to the mediators' distribution at the site. A Chapman-Enskog analysis is performed leading to theoretical predictions of the macroscopic equations inside the transition layer and to the transition-layer thickness. Chapman-Enskog analysis is restricted to near-equilibrium states and was unable to predict the correct second-order interfacial tension dependence on the modeled long-range fields intensity. Interfacial tension was, only, correctly retrieved using a nonequilibrium solution. Theoretical predictions are compared with simulation results and the model is tested considering its ability in describing the dynamical behavior of the interface and Galilean invariance.

DOI: 10.1103/PhysRevE.68.056302 PACS number(s): 47.11.+j

I. INTRODUCTION

Flow of immiscible fluids is, classically, treated by considering that the transition layer has a null thickness and by performing a momentum balance around this layer. At microscopic level, when two immiscible fluids r and b are mixed, the long-range attraction between the molecules of each fluid is the molecular mechanism promoting fluid segregation. Intermolecular forces may be of many different types, including electrostatic forces between permanent dipoles, induction forces between permanent dipoles and induced dipoles, dispersion forces between nonpolar molecules and hydrogen bonds. In the transition region between the two fluids, a molecule is, predominantly, subjected to attractive fields from its own phase that acts as a potential barrier and gives rise to fluid-fluid interfacial tension. In addition, molecules that are found in this transition layer are subject to r-b collisions that try to mix the two fluids and are responsible for r-b diffusion. The thickness of the transition layer is, consequently, controlled by the strength and length of long-range potentials and by cross collisions, r-b.

Theoretical difficulty is strongly increased when these two fluids interact with a solid surface. In fact, the interfacial energies ζ^{rs} and ζ^{bs} between fluids r and b and the surface are the main macroscopic mechanisms governing interface advancing or receding on a solid surface. When interface advances or recedes along a solid surface, dynamic effects will change the contact angle $\theta^{rb/s}$ with respect to its equilibrium value.

Due to the complexity of intermolecular forces and considering their important contribution in defining fluid-fluid and fluid-solid interaction, Boolean lattice gas and lattice Boltzmann appear to be very suitable as downscale methods that can improve the understanding of complex physical phenomena that are very difficult to describe at the hydrodynamic scale.

In this paper, the field mediators concept, described in Ref. [1], is extended for Boltzmann models of immiscible fluids. Mediators are null-mass particles that are emitted from the lattice sites and whose only action is to invert the momentum of lattice particles, simulating a long-range field. When a site **X** can be considered as an attractive center for k particles, $k=r$, b, it will emit mediators of kind k that will be propagated to neighbor sites in the propagation step. Interference of k mediators pull back to site **X**, k particles moving away from **X**. In this way, following very simple emission and interference rules, mediators try to simulate the effect of long-range forces in fluid separation. Particles of kind r in r-b interface which are thrown by collisions toward the b phase will be pulled back to the r phase when they found r mediators in the same site and in the same direction, after propagation step.

Gunstensen *et al.* [2,3] are attributed to be the first who introduced immiscible fluids color based models in the frame of the lattice-Boltzmann method. A more popular two-phase flow model, based on a pseudopotential function, was derived by Shan and Chen [4]. This method was later extended to three dimensions [5]. A drawback in the above model is that it become unstable when used to simulate fluids with very different viscosities (say $\mu_1/\mu_2>7$), as reported in Ref. [6].

In the present work, immiscible fluids r and b are modeled by splitting BGK (Bhatnagar-Gross-Krook) collision term, separately considering r-r and r-b collisions. In fact, it was shown earlier (see, e.g., Philippi and Brun [7]) that the collision term in Boltzmann continuous equation for fluid r can be split into a self, r-r, and a cross, r-b, collision terms. In this way, in contrast with the previous models, viscosity coefficients μ_r and μ_b and binary diffusivity $\mathcal{D}_{rb}$ can be

*Email address: emerich@lmpt.ufsc.br
†Email address: facin@lmpt.ufsc.br
‡Email address: philippi@lmpt.ufsc.br

independently managed using three independent relaxation times. This idea was, recently, applied to miscible fluids [8]. For immiscible fluids flow, interfacial tension is retrieved by modifying *r-b* collision term, introducing long-range forces in the transition layer through the use of field mediators. Mediators' action is restricted to the transition layer and ideal gas state equation is retrieved for each fluid, far from the interface. In this way, we limit ourselves to an athermal model and no attempt to describe phase transitions and their related effects will be given here. The first tentative to a two-phase thermodynamically consistent model was performed by Swift *et al.* [9,10]. In spite of the fact that the development of the free-energy model was inspired by Cahn-Hillard model, it was pointed out that the model cannot lead to correct energy transport [11] and, moreover, it is not Galilean invariant [12]. An invariant Galilean model based on the free-energy model was presented in Ref. [13] to simulate multiphase flows (*not multicomponent*) in two dimensions. More recently, Galilean invariant models based on the free-energy approach were presented in Refs. [14,15]. A detailed comparison among these models has yet to be done.

II. MODEL

In the presently proposed model, considering two immiscible fluids *r* and *b*, long-range attraction between the particles of the same species is simulated by producing field mediators on the lattice sites [1], just before propagation step. Considering $R_i(\mathbf{X},T)$ to be the particles distribution of *r* particles in site $\mathbf{X}$ at time *T* and, similarly, for $B_i(\mathbf{X},T)$, mediators are created just before propagation step, and propagated, following

$$M_i^r(\mathbf{X}+\mathbf{c}_i,T+1) = \alpha M_i^r(\mathbf{X},T)+\beta\frac{\sum_j R_j(\mathbf{X},T)}{\sum_j R_j(\mathbf{X},T)+\sum_j B_j(\mathbf{X},T)}, \tag{1}$$

where $\alpha+\beta=1$.

Equation (1) can be considered as an outgrown of Eq. (37) from the Boolean model proposed in Ref. [1]. The first term on the right-hand side of the above equation is, in fact, a recurrence relation, since $M_i^r(\mathbf{X},T)$ depends on $M_i^r(\mathbf{X}-\mathbf{c}_i,T-1)$ and on $K_j(\mathbf{X}-\mathbf{c}_i,T-1)$, $K=R,B$, for all *j* neighbor sites around site $\mathbf{X}-\mathbf{c}_i$, through second-order terms in α and β. In this way, M_i^r at site $\mathbf{X}$, will be dependent on the next neighbor *r*-particles concentration through first-order terms, on the second neighbor *r* particles through second-order terms, and so on. When $\alpha=0$ (or $\beta=1$), mediators are created at site $\mathbf{X}$, with the solely information of the concentration of *r* particles on next neighbor sites: mediators distribution related to the direction *i* will be given by the mass fraction of *r* particles on site $\mathbf{X}-\mathbf{c}_i$, at time $T-1$. In this case interaction length corresponds to 1 lattice unit. By increasing α with respect to β, interaction length can be, arbitrarily, increased.

Mediators are created at each site $\mathbf{X}$ and propagated with the unitary lattice velocity $\mathbf{c}_i$. Interference of field mediators with lattice particles is described in the following.

Lattice-Boltzmann equation for kind *K* particles is written as

$$K_i(\mathbf{X}+\mathbf{c}_i,T+1)-K_i(\mathbf{X},T) = \Omega(R_0,\ldots,R_{b_m},B_0,\ldots,B_{b_m}), \tag{2}$$

for $K=R,B$. Collision operator Ω_i^k is required to satisfy mass and momentum conservation

$$\sum_{i=0}^{b_m}\Omega_i^r=0, \tag{3}$$

$$\sum_{i=0}^{b_m}\Omega_i^b=0, \tag{4}$$

$$\sum_{i=0}^{b_m}\mathbf{c}_i(\Omega_i^r+\Omega_i^r)=0. \tag{5}$$

A three-parameters BGK collision term that satisfies the above restrictions is proposed in the present work, written as

$$\Omega_i^r=\omega^r\frac{R_i^{eq}(\rho^r,\mathbf{u}^r)-R_i}{\tau^r}+\omega^b\frac{R_i^{eq}(\rho^r,\vartheta^b)-R_i}{\tau^m}, \tag{6}$$

where

$$\rho^k=\sum_{i=0}^{b_m}K_i \tag{7}$$

and

$$\mathbf{u}^k=\frac{1}{\rho^k}\sum_{i=1}^{b_m}K_i\mathbf{c}_i \tag{8}$$

are, respectively, the macroscopic density and velocity of component *k*, $k=r,b$. The ω's in Eq. (6) are the mass fractions, $\omega^k=\rho^k/\rho$.

Equilibrium distributions are considered to be the well known small velocity expansions of $O(u^2)$, appropriated to the description of athermal incompressible flow,

$$R_i^{eq}(\rho^r,\mathbf{u})=\frac{\rho^r}{b}+\frac{D\rho^r}{b_m c^2}c_{i\alpha}u_\alpha+\frac{D(D+2)\rho^r}{2b_m c^4}c_{i\alpha}c_{i\beta}u_\alpha u_\beta - \frac{D\rho^r}{2b_m c^2}(u)^2, \quad i=1,\ldots,b_m, \tag{9}$$

$$R_0^{eq}(\rho^r,\mathbf{u})=\frac{\rho^r}{b}b_0-\frac{\rho^r}{c^2}(u)^2, \tag{10}$$

and similarly for $B_i^{eq}(\rho^b,\mathbf{u})$, where b_m is the number of lattice directions, b_0 is a free integer parameter related to the allowable number of rest particles in Boolean models, $b=b_m+b_0$ and D is the Euclidean lattice dimension

The first term on the right hand side of Eq. (6) is related to the relaxation of r-particles distribution to an equilibrium state given by the r-component density and velocity, considering r-r collisions, only. The second term considers r-b collisions and is related to the relaxation of r-particles to an equilibrium state given by the density ρ^r and by a b velocity

$$\vartheta^b=\mathbf{u}^b-A\hat{\mathbf{u}}^m, \tag{11}$$

modified by the action of r mediators present in the same site. Constant A is to be related to interfacial tension. For ideal miscible fluids [8], $A=0$ and this collision term will describe the relaxation of r-particles distribution to an equilibrium state given by ρ^r and $\mathbf{u}^b$, as a consequence of r-b cross collisions. In immiscible fluids, Eq. (11) means that particles of kind r will be separated from b particles by long-range attractive forces from r phase.

In the same way,

$$\vartheta^r=\mathbf{u}^r+A\hat{\mathbf{u}}^m. \tag{12}$$

In Eqs. (11) and (12),

$$\hat{\mathbf{u}}^m=\begin{cases}\dfrac{\mathbf{u}^m}{|\mathbf{u}^m|} & \text{when } \mathbf{u}^m\neq 0\\ 0 & \text{when } \mathbf{u}^m=0,\end{cases} \tag{13}$$

where mediators velocity at site $\mathbf{X}$ is given by

$$\mathbf{u}^m=\sum_{i=1}^{b_m}(M_i^r-M_i^b)\mathbf{c}_i, \tag{14}$$

pointing to the same direction where r mediators were propagated, i.e., to the b phase.

In the present model, since $|\hat{\mathbf{u}}^m|=\{0,1\}$, the long-range effect on the cross-collision part of Ω_i^r is to relax r-particles distribution to an equilibrium distribution with a $\mathbf{u}^b$ velocity, modified, in all lattice sites inside lattice domains where r and b particles are simultaneously found, by a vector whose modulus is constant and equal to A. This is not the only choice for satisfying the restrictions on *local* mass and momentum preservation, but the simplest one and, although this could appear as a model's restriction, the *direction* of $\hat{\mathbf{u}}^m$ in a given site $\mathbf{X}$ will be dependent on the mediators distribution M_i^r and M_i^b in that site and these distributions are dependent on r and b particles distributions in the neighbor sites at the previous time steps.

III. CHAPMAN-ENSKOG ASYMPTOTIC ANALYSIS IN THE TRANSITION LAYER

In pure phases the interference between field mediators and lattice particles has null effect, as a consequence of momentum preservation. In this way, far from the interface, pressure P^k is directly related to density ρ^k, $k=r,b$, through the square of sound speed $c_s^2=(b_m c^2)/(bD)$ and macroscopic Navier-Stokes equations are retrieved for incompressible flow [16]. In this way, Chapman-Enskog analysis will be, here, restricted to the transition layer.

Consider that, at equilibrium, the species r and b are well mixed in their entire spatial domain. In this condition, long-range effects are null and $\mathbf{u}^r=\mathbf{u}^b=\mathbf{u}$, where $\mathbf{u}$ is the mixture velocity $\mathbf{u}=\omega^r\mathbf{u}^r+\omega^b\mathbf{u}^b$. Equllibrium distributions are given by Eqs. (9) and (10). Consider, also, that the long-range field strength, described by factor A in present model, is weak enough to produce only small deviations from $R_i^{eq}(\rho^r,\mathbf{u})$ and $B_i^{eq}(\rho^b,\mathbf{u})$. In this way, fluid segregation can be considered to be a first-order perturbation effect on the equilibrium state given by Eqs. (9) and (10) and interfacial thickness L can be regarded as large enough ($L\to\infty$ when $A\to 0$) to enable Chapman-Enskog analysis, by considering the length 1 corresponding to a lattice unit as much smaller than the interfacial thickness L, in lattice units, i.e., by considering the Knudsen number $\mathcal{K}_n=1/L\to 0$. Obviously, this, also, implies to consider that the long-range strength factor A has the same order of magnitude of $\mathcal{K}_n$. A nonequilibrium distribution is proposed in Sec. VI, when A is arbitrary and L corresponds to some few lattice units.

Distribution $K_i(\mathbf{X},T)$ is expanded in powers of a small parameter that, in the present case, can, indifferently, be chosen as A or $\mathcal{K}_n$,

$$K_i=K_i^0+\mathcal{K}_nK_i^1+\cdots,\quad K=R,B,\quad i=0,1,\ldots,b_m, \tag{15}$$

and the time derivative has an induced decomposition

$$\partial_t=\partial_o+\mathcal{K}_n\partial_1+\cdots. \tag{16}$$

The collision term given by Eq. (6) can be expanded around $R_i^{eq}(\rho^r,\mathbf{u})$, giving

$$\begin{aligned}\Omega_i^r=&\left(\frac{\omega^r}{\tau^r}+\frac{\omega^b}{\tau^m}\right)[R_i^{eq}(\rho^r,\mathbf{u})-R_i]+\left(\frac{\omega^r}{\tau^r}-\frac{\omega^b}{\tau^m}\right)\rho^r\frac{D}{b_m c^2}\\ &\times\left[\mathbf{c}_i-\mathbf{u}+\frac{(D+2)}{c^2}(\mathbf{c}_i\cdot\mathbf{u})\mathbf{c}_i\right]\cdot(\mathbf{u}^r-\mathbf{u})\\ &-\rho\frac{\omega^r\omega^b}{\tau^m}A\frac{D}{b_m c^2}\left[\mathbf{c}_i-\mathbf{u}+\frac{(D+2)}{c^2}(\mathbf{c}_i\cdot\mathbf{u})\mathbf{c}_i\right]\cdot\hat{\mathbf{u}}^m\\ &+O((\mathbf{u}^r-\mathbf{u})^2,A(\mathbf{u}^r-\mathbf{u}),\ldots),\end{aligned} \tag{17}$$

and, similarly, for Ω_i^b.

Writing lattice-Boltzmann equation, Eq. (2), in continuous variables using dimensionless variables $t^*=t/t_c$, where t_c is a macroscopic time, $\mathbf{r}^*=\mathbf{r}/L$, and using Eqs. (15) and (16),

$$\frac{\epsilon}{\mathcal{K}_n}\partial_{o*}R_i^0+c_{i\alpha}\partial_{\alpha*}R_i^o+\mathcal{K}_n\left[\begin{array}{l}\dfrac{\epsilon}{\mathcal{K}_n}\partial_{o*}R_i^1+\dfrac{\epsilon}{\mathcal{K}_n}\partial_{1*}R_i^o+c_{i\alpha}\partial_{\alpha*}R_i^1\\ +\dfrac{1}{2}\left(\dfrac{\epsilon}{\mathcal{K}_n}\right)^2\partial_{o*o*}R_i^o+\dfrac{1}{2}c_{i\alpha}c_{i\beta}\partial_{\alpha*\beta*}R_i^o+\dfrac{\epsilon}{\mathcal{K}_n}c_{i\alpha}\partial_{o*}\partial_{\alpha*}R_i^o\end{array}\right]+\cdots$$

$$=\frac{1}{\mathcal{K}_n}\left(\frac{\omega^r}{\tau^r}+\frac{\omega^b}{\tau^m}\right)[R_i^{eq}(\rho^r,\mathbf{u})-R_i^o]-\left(\frac{\omega^r}{\tau^r}+\frac{\omega^b}{\tau^m}\right)R_i^1+\left(\frac{\omega^r}{\tau^r}-\frac{\omega^b}{\tau^m}\right)\rho^r\frac{D}{b_mc^2}\left[\mathbf{c}_i-\mathbf{u}+\frac{(D+2)}{c^2}(\mathbf{c}_i\cdot\mathbf{u})\mathbf{c}_i\right]\cdot\mathbf{j}^{r,1}$$

$$-\rho\frac{\omega^r\omega^b}{\tau^m}\frac{A}{\mathcal{K}_n}\frac{D}{b_mc^2}\left[\mathbf{c}_i-\mathbf{u}+\frac{(D+2)}{c^2}(\mathbf{c}_i\cdot\mathbf{u})\mathbf{c}_i\right]\cdot\hat{\mathbf{u}}^m-\mathcal{K}_n\left(\frac{\omega^r}{\tau^r}+\frac{\omega^b}{\tau^m}\right)R_i^2+\mathcal{K}_n\left(\frac{\omega^r}{\tau^r}-\frac{\omega^b}{\tau^m}\right)\rho^r\frac{D}{b_mc^2}$$

$$\times\left[\mathbf{c}_i-\mathbf{u}+\frac{(D+2)}{c^2}(\mathbf{c}_i\cdot\mathbf{u})\mathbf{c}_i\right]\cdot\mathbf{j}^{r,2}+\cdots, \tag{18}$$

where $\epsilon=\delta/t_c$ is the ratio between the time δ expended for a particle to travel a single lattice unit and the macroscopic time t_c, or, equivalently, $\epsilon=1/t_c$, when t_c is considered in lattice units. Flux

$$\mathbf{j}^{k,s}=\sum_i K_i^s\mathbf{c}_i, \quad k=r,b, \tag{19}$$

is the sth order contribution to species k diffusive flux

$$\mathbf{j}^r=\rho^r(\mathbf{u}^r-\mathbf{u})=\mathcal{K}_n\mathbf{j}^{r,1}+\mathcal{K}_n^2\mathbf{j}^{r,2}+\cdots. \tag{20}$$

In Eq. (18), the first term in the second member will be dominant when $\epsilon\ll\mathcal{K}_n\ll1$, corresponding to the low Mach number incompressible limit.

The solution of

$$\left(\frac{\omega^r}{\tau^r}+\frac{\omega^b}{\tau^m}\right)[R_i^{eq}(\rho^r,\mathbf{u})-R_i]=0, \tag{21}$$

gives the zeroth-order solution to R_i,

$$R_i^o=R_i^{eq}(\rho^r,\mathbf{u}). \tag{22}$$

Using the same reasoning for species b,

$$B_i^o=B_i^{eq}(\rho^b,\mathbf{u}). \tag{23}$$

In the first order, R_i^1 is the solution of

$$\frac{\epsilon}{\mathcal{K}_n}\partial_{o*}R_i^o+c_{i\alpha}\partial_{\alpha*}R_i^o$$

$$=-\left(\frac{\omega^r}{\tau^r}+\frac{\omega^b}{\tau^m}\right)R_i^1+\left(\frac{\omega^r}{\tau^r}-\frac{\omega^b}{\tau^m}\right)\frac{D}{b_mc^2}$$

$$\times\left[\mathbf{c}_i-\mathbf{u}+\frac{(D+2)}{c^2}(\mathbf{c}_i\cdot\mathbf{u})\mathbf{c}_i\right]\cdot\mathbf{j}^{r,1}$$

$$\times-\rho\frac{\omega^r\omega^b}{\tau^m}\frac{A}{\mathcal{K}_n}\frac{D}{b_mc^2}$$

$$\times\left[\mathbf{c}_i-\mathbf{u}+\frac{(D+2)}{c^2}(\mathbf{c}_i\cdot\mathbf{u})\mathbf{c}_i\right]\cdot\hat{\mathbf{u}}^m, \tag{24}$$

giving

$$\left(\frac{\omega^b}{\tau^m}+\frac{\omega^r}{\tau^r}\right)R_i^1=\left(\frac{\omega^r}{\tau^r}-\frac{\omega^b}{\tau^m}\right)\frac{D}{b_mc^2}$$

$$\times\left[c_{i\alpha}-u_\alpha+\frac{(D+2)}{c^2}(c_{i\beta}u_\beta)c_{i\alpha}\right]j_\alpha^{r,1}$$

$$-\rho\frac{\omega^r\omega^b}{\tau^m}\frac{A}{\mathcal{K}_n}\frac{D}{b_mc^2}$$

$$\times\left[c_{i\alpha}-u_\alpha+\frac{(D+2)}{c^2}(c_{i\beta}u_\beta)c_{i\alpha}\right]\hat{u}_\alpha^m$$

$$-\frac{1}{b}\rho\omega^r\partial_{\alpha*}u_\alpha-\frac{D}{b_mc^2}\rho\omega^r\partial_{\alpha*}u_\beta c_{i\alpha}c_{i\beta}$$

$$+\frac{1}{b}\rho u_\alpha\partial_{\alpha*}\omega^r+\frac{1}{b}c_{i\alpha}\partial_{\alpha*}\omega^r$$

$$+\frac{D}{b_mc^2}c_{i\alpha}c_{i\beta}\rho u_\beta\partial_{\alpha*}\omega^r. \tag{25}$$

A similar expression can be obtained for B_i^1.

IV. MACROSCOPIC EQUATIONS INSIDE THE TRANSITION LAYER

At $\mathcal{K}_n$ zeroth order mass conservation equation is obtained by adding all the i-contributions given by Eq. (24),

$$\partial_o\rho^r+\partial_\alpha(\rho^r u_\alpha)=0. \tag{26}$$

In the same way, Euler's equation is retrieved at this order, given by,

$$\partial_o(\rho u_\alpha)+\partial_\beta(P\delta_{\alpha\beta}+\rho u_\alpha u_\beta)=0, \tag{27}$$

where $P=\rho c_s^2$.

Equation (25) can be used to give the first-order contribution to the species-r diffusive flux, Eq. (19). The time derivatives $\partial_1(\rho^r)$ and $\partial_1(\rho\mathbf{u})$ are obtained by considering the mass and velocity moments of the terms that appear in Eq. (18) multiplied by the Knudsen number $\mathcal{K}_n$. The final form of the macroscopic equations are obtained by retrieving the time derivatives of ρ^r and $\rho\mathbf{u}$ from Eq. (16), and are presented below.

Mass conservation equation for the r species is written as

$$\partial_t\rho^r+\partial_\alpha(\rho^r u_\alpha)+\partial_\alpha(j_\alpha^r)=0, \tag{28}$$

where

$$\mathbf{j}^r=(\mathbf{j}^r)^{dif}+(\mathbf{j}^r)^{lrf} \tag{29}$$

and

$$(\mathbf{j}^r)^{dif}=-\frac{b_m c^2}{bD}\left(\tau^m-\frac{1}{2}\right)\rho\nabla\omega^r, \tag{30}$$

is the r-species ordinary Fickean diffusive flux, promoted by concentration gradients and,

$$(\mathbf{j}^r)^{lrf}=-\rho\omega^r\omega^b A\hat{\mathbf{u}}^m, \tag{31}$$

corresponds to the long-range action on component r.

In this way, Fickean diffusion that would promote mixing between species r and b, enlarging the interface thickness is counterbalanced by long-range forces, which act in the opposed way, pulling back r particles that are thrown out of their own phase by collisions with b particles. In fact, dynamic equilibrium between Fickean diffusion and long-range action giving a null $\mathbf{j}^r$ flux is a necessary condition for interface stability. The lacking of energy conservation in the present model restricts the analysis to the low-velocity, incompressible limit. Choosing $b_m/b=D/(D+2)$, Chapman-Enskog analysis leads to the following momentum equation:

$$\partial_t(\rho u_\alpha)+\partial_\beta(P_{\alpha\beta}+\rho u_\alpha u_\beta) = \eta\partial_\beta[\rho(\partial_\alpha u_\beta+\partial_\beta u_\alpha)]-\partial_\beta[W(\omega_r)(j_\alpha^r u_\beta+j_\beta^r u_\alpha)], \tag{32}$$

where

$$W(\omega_r)=\frac{\dfrac{\omega^r}{\tau^r}-\dfrac{\omega^r}{\tau^m}+\dfrac{1}{2\tau^m}}{\dfrac{\omega^r}{\tau^r}+\dfrac{\omega^b}{\tau^m}}-\frac{\dfrac{\omega^b}{\tau^r}-\dfrac{\omega^b}{\tau^m}+\dfrac{1}{2\tau^m}}{\dfrac{\omega^b}{\tau^b}+\dfrac{\omega^r}{\tau^m}}. \tag{33}$$

The kinematic viscosity coefficient η, in lattice units, is given by

$$\eta=\frac{c^2}{D+2}\left[\frac{1}{2}-\left(\frac{\omega^r}{\dfrac{\omega^r}{\tau^r}+\dfrac{\omega^b}{\tau^m}}+\frac{\omega^b}{\dfrac{\omega^b}{\tau^b}+\dfrac{\omega^r}{\tau^m}}\right)\right]. \tag{34}$$

Mixture viscosity appears as a function of the three collision parameters, τ^r, τ^b, τ^m and the mass fractions, ω^r,ω^b. Due to local momentum conservation, viscosity coefficient is identical to the viscosity coefficient that was found for ideally miscible fluids [8]. In addition, when $\omega^r\to 1$,

$$\eta=\frac{c^2}{D+2}\left(\tau^r-\frac{1}{2}\right), \tag{35}$$

which is the correct expression for the kinematic viscosity of pure component r.

As commented above, the second term on the right hand side of Eq. (32) is null for stable interfaces, when $\mathbf{j}^r=\mathbf{j}^b=0$.

Pressure $P_{\alpha\beta}$ is given by

$$P_{\alpha\beta}=\rho c_s^2\delta_{\alpha\beta}+\rho\omega^r\omega^b\left(\frac{\tau^r}{\omega^r\tau^m+\omega^b\tau^r}-\frac{\tau^b}{\omega^b\tau^m+\omega^r\tau^b}\right) \times(\hat{u}_\alpha^m u_\beta+\hat{u}_\beta^m u_\alpha)A, \tag{36}$$

in this way pressure $P_{\alpha\beta}$ inside the interface follows ideal gas law $P=\rho c_s^2\delta_{\alpha\beta}$, with an $O(Au)$ velocity dependent, deviation. Although momentum equation remains invariant by a Galilean group of transformations, this deviation is *unphysical* since it produces a velocity dependent interfacial tension. Since $A\sim\mathcal{K}_n$, this error is expected to be meaningless, when interface velocity $\mathbf{u}$ is small. In addition, this effect has its magnitude decreased when relaxation parameters τ^r and τ^b are close (see Sec. VII).

In Sec. VII using a nonequilibrium solution, for the special case where interfacial velocity $\mathbf{u}=0$, it is shown that interfacial tension is related to an A^2 term, which could only be retrieved in the present *near-equilibrium* analysis by performing an $O(Kn^2)$ Chapman-Enskog analysis, which is outside the scope of the present work.

In this manner when long-range factor A is small enough and neglecting the $O(Au)$ and $O(A^2)$ factors, we can conclude that, inside the interface, r-b mixture behaves as an ideal mixture, following Navier-Stokes momentum equations for incompressible flows. With these approximations we are, also, forced to conclude that interfacial tension is null. This is an unphysical result and reveals the weakness of present first-order Chapman-Enskog analysis for the interface region between two immiscible fluids. Further considerations will be given in Sec. VII.

V. TRANSITION-LAYER THICKNESS

Restricting the analysis to a plane interface and taking coordinate y normal to the interface, the stability condition may be expressed as

$$\frac{b_m c^2}{bD}\left(\tau^m-\frac{1}{2}\right)\rho\frac{d}{dy}(\omega^r)=\rho\omega^r(1-\omega^r)A, \tag{37}$$

since $\hat{u}_y^m=-1$ for all the sites inside the interface.

Above equation may be integrated along the interfacial thickness, giving

$$L=\frac{c_s^2\left(\tau^m-\frac{1}{2}\right)}{A}\int_0^1\frac{d\omega^r}{\omega^r(1-\omega^r)}. \tag{38}$$

As it was to be expected, transition-layer thickness is proportional to the ratio τ^m/A, i.e., to the ratio between the r-b cross-collision factor τ^m, related to the Fickean diffusivity $\mathcal{D}$ and the long-range intensity A. When A is increased with respect to $\mathcal{D}$, transition-layer thickness is decreased. The integral above, Eq. (38), diverges when ω^r is considered between the limits 0 and 1. This is consistent with the fact that, in the continuum limit, transition layer has an infinite thickness. For practical purposes, the integral, Eq. (38), can be calculated between appropriate limits ω_0^r and ω_L^r, giving finite values for the transition-layer thickness.

VI. NONEQUILIBRIUM SOLUTION

When long-range strength factor A increases, the interfacial thickness L can have some few lattice units and Chapman-Enskog analysis is no longer possible. Distributions R_i and B_i cannot be considered as close to their equilibrium counterparts given by Eqs. (9) and (10) and *nonequilibrium* solutions satisfying lattice-Boltzmann equations must be searched. This is a very difficult problem and was only solved, in the present paper, in the special case when the interface velocity $\mathbf{u}$ is null.

Consider R_i^*, B_i^* to be such nonequilibrium solutions. When the interface is at rest, R_i^*, B_i^* are, also, *stationary*. In this case, stability condition for the interface requires

$$R_i^{*\prime}=R_{-i}^*, \tag{39}$$

for avoiding diffusion of the r particles into the b phase. In fact, in stationary conditions, particle distributions are independent of time: the flux of particles of kind r that are found in direction i, after collision and which will be propagated to the direction i of the site $\mathbf{X}+\mathbf{c}_i$ and found in this site at time $T+1$, must be canceled by the flux of particles found in the direction $-i$ of site $\mathbf{X}$ that propagate from site $\mathbf{X}+\mathbf{c}_i$ at time $T-1$. A similar reasoning applies to the b component.

Stability condition, Eq. (39), means that

$$R_i^{*\prime}=R_i^*+\omega^r\frac{R_i^{eq}(\rho^r,\mathbf{u}^r)-R_i^*}{\tau^r}+\omega^b\frac{R_i^{eq}(\rho^r,\vartheta^b)-R_i^*}{\tau^m}=R_{-i}^*, \tag{40}$$

which enables to find

$$\left(\frac{\omega^r}{\tau^r}+\frac{\omega^b}{\tau^m}\right)R_i^*=\omega^r\frac{R_i^{eq}(\rho^r,\mathbf{u}^r)}{\tau^r}+\omega^b\frac{R_i^{eq}(\rho^r,\vartheta^b)-R_i^*}{\tau^m}+(R_i^*-R_{-i}^*), \tag{41}$$

for $i=0,\ldots,b_m$. An explicit form for $R_i^*-R_{-i}^*$ may be obtained by calculating R_{-i}^* from Eq. (41) and by subtracting the resulting equation from Eq. (41):

$$R_i^*-R_{-i}^*=\frac{1}{\left(\frac{\omega^r}{\tau^r}+\frac{\omega^b}{\tau^m}-2\right)}\left[2\frac{\omega^r}{\tau^r}\frac{D}{b_m c^2}\rho^r\mathbf{u}^r\cdot\mathbf{c}_i+2\frac{\omega^b}{\tau^m}\frac{D}{b_m c^2}\rho^r(\mathbf{u}^b-A\hat{\mathbf{u}}^m)\cdot\mathbf{c}_i\right]. \tag{42}$$

Above solution, Eq. (41), is, in fact, a nonequilibrium solution that depends on the relaxation times and on the long-range strength factor A. When the interface is moving with a constant velocity, the correct stability condition to be used is

$$\sum R_i^{*\prime}\mathbf{c}_i-\sum R_{-i}^*\mathbf{c}_i=2\rho^r\mathbf{u}, \tag{43}$$

but this condition, used in conjunction with the mass and momentum conservation conditions, does not lead to a *unique* solution for R_i^* and the problem remains, still, open.

VII. INTERFACIAL TENSION

Restricting the analysis to a plane interface and taking coordinate y normal to the interface, interfacial tension σ_{rb} was calculated, using

$$\sigma_{rb}=\int_{-\infty}^{\infty}[\Pi_{yy}^*(y)-\Pi_{xx}^*(y)]dy, \tag{44}$$

where the momentum fluxes are given by

$$\Pi_{yy}^*=\sum_i(R_i^*+B_i^*)c_{iy}c_{iy}=c_s^2\rho+\rho A^2 a_r a_{r1}+\rho A^2 a_b a_{b1}, \tag{45}$$

$$\Pi_{xx}^*=\sum_i(R_i^*+B_i^*)c_{ix}c_{ix}=c_s^2\rho, \tag{46}$$

and

$$a_r=\frac{\omega^r(\omega^r-1)}{(\omega^r\tau^m+\tau^r-\omega^r\tau^r)(2\tau^m-1)}, \tag{47}$$

$$a_b=\frac{\omega^r(\omega^r-1)}{(\omega^r\tau^m+\tau^m-\omega^r\tau^b)(2\tau^m-1)}, \tag{48}$$

$$a_{r1}=\frac{-\omega^r\tau^m+(\omega^r)^2\tau^m-(\omega^r)^2\tau^r+2\omega^r\tau^r-4\omega^r\tau^r\tau^m-\tau^r+4\tau^r\tau^m-4\tau^r(\tau^m)^2}{2\tau^m-1}, \tag{49}$$

$$a_{b1}=\frac{-\omega^r\tau^m+(\omega^r)^2\tau^m-(\omega^r)^2\tau^b+4\omega^r\tau^b\tau^m-4\tau^b(\tau^m)^2}{2\tau^m-1}. \tag{50}$$

A closed form expression for the interfacial tension is obtained, in terms of lattice parameters and relaxation times by changing $y\rightarrow\omega^r$ variables, considering that at each point **X** of the interface the diffusive flux of r (or b) particles promoted by concentration gradients must be cancealed by long-range forces, i.e., by using Eq. (37). This results in,

$$\sigma_{rb}=c_s^2\left(\tau^m-\frac{1}{2}\right)A\rho_{out}\int_0^1(a_ra_{r1}+a_ba_{b1})\frac{d\omega^r}{\omega^r(1-\omega^r)}, \tag{51}$$

where ρ_{out} is the particles density outside the transition layer.

The changing variables $y\rightarrow\omega^r$ were possible imposing null mass flux through interface.

When the interfacial velocity $u\neq0$, we have used Eq. (36) from Sec. IV, for estimating the deviation in the interfacial tension produced by a finite interfacial velocity, using the same above procedure. For a plane interface moving with a speed u it was concluded that

$$\Delta(\sigma_{rb})_u=2\rho_{out}c_s^2\left(\tau^m-\frac{1}{2}\right)u\left(\frac{\tau^r}{\tau^r-\tau^m}\ln\frac{\tau^m}{\tau^r}+\frac{\tau^b}{\tau^m-\tau^b}\ln\frac{\tau^m}{\tau^b}\right). \tag{52}$$

In the above expression, the factor between parenthesis in the right member is always non-negative and is null when $\tau^r=\tau^b$, i.e., when r and b fluids have the same viscosity.

VIII. COMPARISON BETWEEN THEORETICAL PREDICTION AND SIMULATION RESULTS

All numerical simulations were performed setting $\alpha=0$ and $\beta=1$, using a D3Q19 lattice.

A. Pressure distribution inside the transition layer

Equal volumes of r and b fluids were distributed on a three-layer chamber $100\times100\times3$, respectively, on the left and right sides of the chamber. Periodic conditions were used for the upper and down and front and back chamber surfaces. Bounce-back conditions restrict fluid velocity to zero at the left and right chamber surfaces. At $t=0$ long-range forces are applied and simulation starts.

Figure 1 shows the pressure distribution inside the transition layer, calculated using Eqs. (45) and (46), and measured after simulation has reached the equilibrium. Simulation parameters are $\tau^r=1$, $\tau^b=1$, $\tau^m=2$, $A=0.5$. Normal and tangential pressures are found by measuring the momentum exchanged between the lattice particles and a surface placed, respectively, at vertical (normal to y) and horizontal position, for each point along the median line crossing the interface. Agreement between theoretical and simulated values is excellent. In the transition layer, pressure deviates from ideal gas law, i.e., $P=c_s^2\rho$, from a positive factor that is proportional to the long-range intensity factor A [see Eq. (45)] and, for each y inside the transition layer, this factor is the difference between the full black and the trace lines shown in Fig. 1.

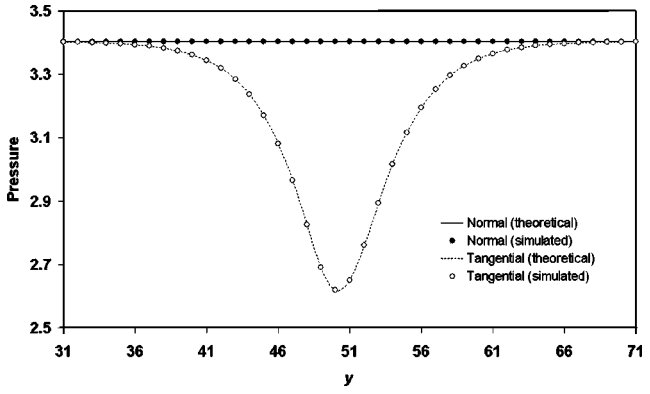

FIG. 1. Pressure distribution inside the transition layer (in lattice units). The parameters are $\rho=10$, $\tau^r=1$, $\tau^b=1$, $\tau^m=2$, and $A=0.5$.

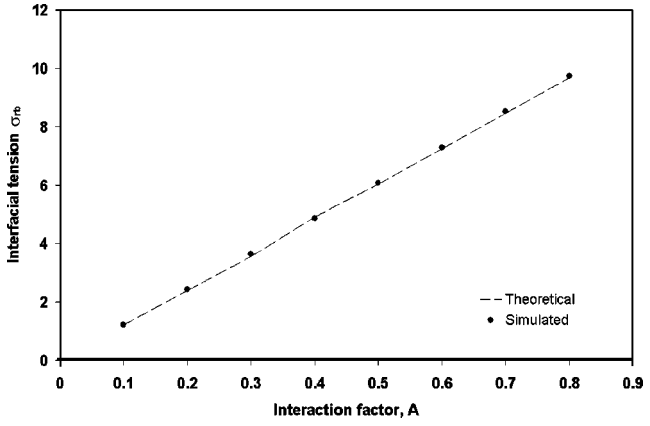

FIG. 2. Comparison between theoretical prediction and simulated results for σ_{rb} (in lattice units). The density was set $\rho=10$ and the relaxation times $\tau^r=1$, $\tau^b=3$, and $\tau^m=1.5$.

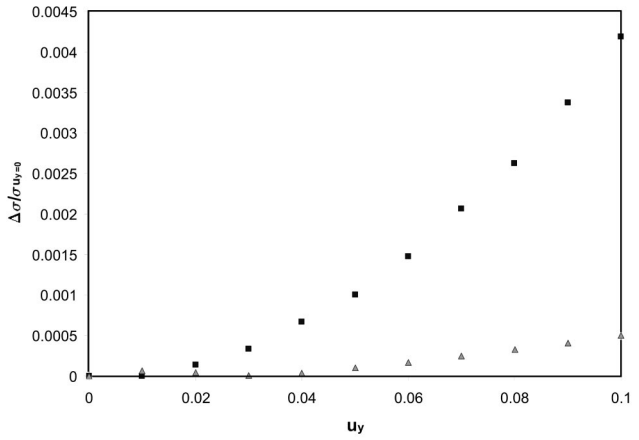

FIG. 3. Dependence of σ_{rb} on the velocity (in lattice units). The density was set $\rho=1$ and the relaxation times $\tau^r=0.6$, $\tau^b=2$, and $\tau^m=1.0$. Black squares are the results using $A=0.4$ and triangles represent results using $A=0.2$.

B. Interfacial tension

Figure 2 gives a comparison between theoretical prediction, Eq. (51), and simulated results for the interfacial tension. Simulated results were obtained by adding all the contributions to normal pressure deviation across the interface. When collision parameters τ are kept constant, simulation shows a linear dependence of σ_{rb} with respect to A, also predicted by theoretical analysis [Eq. (51)]. The dependence of the interfacial tension on the velocity can be seen in Fig. 3, giving the results of ten numerical simulations. In each simulation, the velocity u_y was imposed constant on the whole domain. Very different values of the relaxation times were chosen in order to achieve large variations on the interfacial tension ($\tau^r=0.6$, $\tau^b=2.0$, and $\tau^m=1.0$). The graph shows the variation of the interfacial tension with respect to the interfacial tension that is predicted when the interfacial velocity is zero ($\Delta\sigma=\sigma_{u_y=0}-\sigma$). Comparing the simulated results for the dependence of the interfacial tension σ_{rb} with the interfacial velocity u_y, it is possible to see that the linear dependence predicted by Eq. (52) is only fairly true when long-range factor A is small (and second-order factors are negligible). In general there is a u^2 dependence of σ_{rb}. In both simulations ($A=0.2$ and $A=0.4$) the variation of σ_{rb} with **u** was not important, remaining lower than 0.5%.

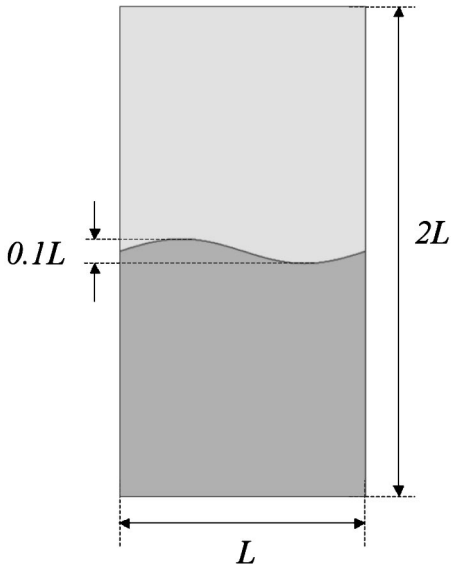

FIG. 4. Initial condition for the simulation of capillary waves.

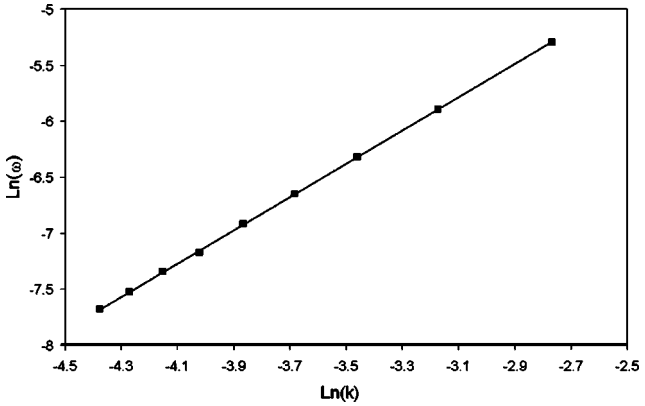

FIG. 5. Dispersion relation of capillary waves, the dashed line is the best fit. The parameters are $\tau^r=\tau^b=0.52$, $\tau^m=1.0$, and $A=0.4$.

C. Capillary waves

The dispersion of capillary waves has been used in order to test the surface-tension dynamics of the lattice Boltzmann models for multiphase flows (see Refs. [2,17,9,18,6]). Following these authors we simulate the decay of capillary waves. The simulations were carried out in rectangular domains (see Fig. 4), measuring $L\times 2L$, with walls at the top

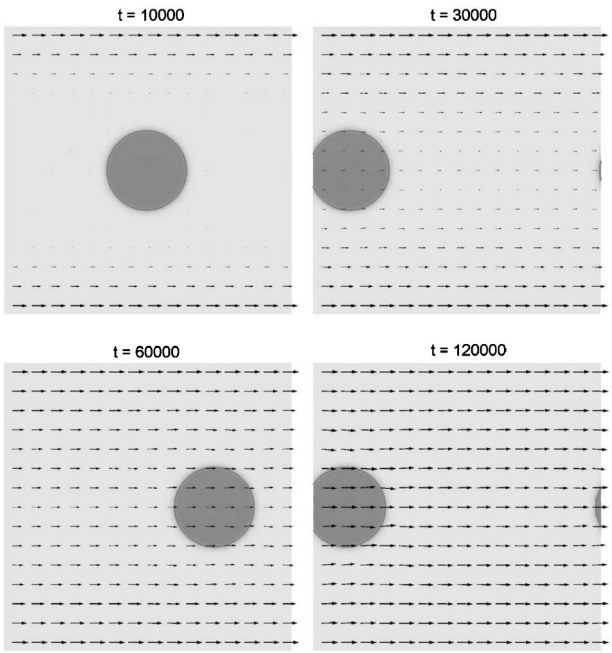

FIG. 6. Evolution of a droplet left in a moving tube. The parameters are $\tau^r=\tau^b=0.6$, $\tau^m=1$, and $A=0.4$.

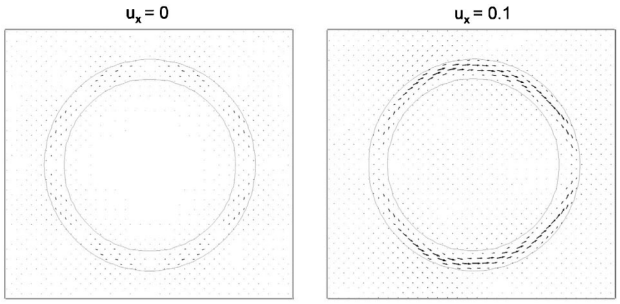

FIG. 7. Measured velocity field in droplet flow, showing spurious currents in the transition layer. Right: droplet at rest in a static frame of reference. Left: droplet moving with a constant velocity observed in a reference frame with the same velocity. The parameters are $\tau^r=\tau^b=0.8$, $\tau^m=1$, and $A=0.4$.

$(y=2L)$ and bottom $(y=0)$ of the box and periodic boundary conditions in the other direction. The region $y>L$ was filled with *r* fluid and $y<L$ with *b* fluid. A sinusoidal wave with amplitude *a*, $a \ll L$ was imposed as initial condition to the interface. An analytical treatment, considering ideal fluids, is known [19] and gives the relation

$$\omega^2=\frac{\sigma k^3}{2\rho}, \tag{53}$$

where *k* is a wave number.

Figure 5 shows the results of nine simulations with *L* varying from 100 to 500. The relaxation times were set $\tau^r=\tau^b=0.52$ and $\tau^m=1.0$, and the interaction factor $A=0.4$. The best fit line has gradient equal to 1.485, an error of 1% with respect the prediction of Eq. (53).

D. Galilean invariance

In Sec. IV it was seen that present Chapman-Enskog analysis was unable to predict the A^2 dependence of the interfacial tension σ_{rb}. In addition, the nonequilibrium analysis given in Sec. VI was restricted to the case when *r*-*b* interface is at rest. In this way, Galilean invariance of the macroscopic equations, inside the transition layer, could not be assured by theoretical means. In order to test the Galilean invariance of the model, the flow of a droplet in a moving tube was simulated. A circular droplet with diameter $D=40$ is put in the center of a domain with 135×135 sites. The droplet is brought to equilibrium at rest. A constant velocity $u_x=0.1$ is, then, imposed at the top and bottom sides, and periodic boundary conditions are used in the *x* direction. The evolution is shown in Fig. 6: when stationary conditions are reached the droplet retrieves its circular shape and the same velocity of the walls. Similar results are presented in Refs. [13,14], in these papers also results using the model proposed by Swift *et al.* [9,10] where the droplet acquires an eliptic shape are shown. Although, at first sight, present results seem to indicate Galilean invariance, a more detailed look at the velocity field shows that this is not a correct conclusion. Indeed, it was shown that spurious currents inside the transition layer are intensified under a constant velocity field. This can be observed in Fig. 7. Spurious currents are due to the lattice discreteness and, apparently, cannot be avoided in lattice-Boltzmann simulation. Nevertheless, in the present case, when the reference frame is moving with a constant speed $u_x=0.1$ (Fig. 7, left), spurious currents are intensified with respect to Fig. 7, right, when they are measured in this moving reference frame. However, as it can be seen in the same figure, this spurious currents enhancement does not affect, significantly, the velocity field in the inner and outer droplet regions, outside the interface and, apparently, good results can be achieved provided that the interfacial region is made small enough, using sufficiently large domains.

IX. CONCLUSION

In the present paper, a lattice-Boltzmann model is proposed for immiscible fluids. Collision term was split, taking mutual and cross collisions into account. Relaxation times were made concentration dependent, considering the very large concentration gradients in the transition layer of immiscible fluids. Long-range forces were simulated by using field mediators. Although macroscopic equations were correctly retrieved inside the transition layer, Knudsen first-order, Chapman-Enskog analysis was unable to predict the $O(A^2)$ dependence of the interfacial tension σ with the long-range factor *A*. In this way, a nonequilibrium solution was necessary, restricted in the present paper to the case when the interfacial velocity $\mathbf{u}=0$. Simulation results and theoretical predictions for σ compare well for all long-range intensity factor values that were used, when $\mathbf{u}=0$. A weak linear dependence of σ with the interfacial velocity was predicted from Chapman-Enskog analysis. Numerical simulations showed that the interfacial tension has, indeed, an $O(u^2)$ dependence. Nevertheless, even in the worst case, when relaxation factors are very different and *A* and *u* values are in the upper simulation limits, this dependence remained smaller than 0.5%. Dynamical behavior of the present model was tested considering the dispersion of capillary waves. Simulation results compare well with classical, theoretical, predictions for the dispersion relation. Finally, Galilean invariance of the present model was verified, considering the behavior of a two-dimensional droplet under a uniform velocity field. No appreciable shift from the initial droplet circular shape was observed, when steady-state conditions were reached. Nevertheless, discreteness produced spurious currents in the transition layer were intensified.

ACKNOWLEDGMENTS

This work was supported by CNPq (Brazilian Council of Scientifical and Technological Development), ANP (Brazilian National Agency of Petroleum), and Finep (Fundação Nacional de Estudos e Pesquisas).

[1] L.O.E. dos Santos and P.C. Philippi, Phys. Rev. E **65**, 046305 (2002).
[2] A.K. Gunstensen, D.H. Rothman, S. Zaleski, and G. Zanetti, Europhys. Lett. **43**, 4320 (1991).
[3] A.K. Gunstensen, D.H. Rothman, S. Zaleski, and G. Zanetti, Europhys. Lett. **18**, 157 (1992).
[4] X. Shan and H. Chen, Phys. Rev. E **47**, 1815 (1993).
[5] N.S. Martys and H. Chen, Phys. Rev. E **53**, 743 (1996).
[6] J. Chin, E.S. Boek, and P. Coneney, Philos. Trans. R. Soc. London, Ser. B **360**, 547 (2002).
[7] P.C. Philippi and R. Brun, Physica A **105**, 147 (1981).
[8] P.C. Facin, P.C. Philipi, and L.O.E. dos Santos, in *Computational Science-ICCS 2003*, Lecture Notes in Computer Science Vol. 2657 (Springer-Verlag, Berlin, 2003), LNCS 2657, pp. 1007–1014.
[9] M.R. Swift, W.R. Osborn, and J.M. Yeomans, Phys. Rev. Lett. **75**, 830 (1995).
[10] M.R. Swift, E. Orlandini, W.R. Osborn, and J.M. Yeomans, Phys. Rev. E **54**, 5041 (1996).
[11] L.S. Luo, Phys. Rev. Lett. **81**, 1618 (1998).
[12] A.D. Angelopoulos, V.N. Paunov, V.N. Burganos, and A.C. Payatakes, Phys. Rev. E **57**, 3237 (1998).
[13] T. Inamuro, N. Konishi, and F. Ogino, Comput. Phys. Commun. **129**, 32 (2000).
[14] A.N. Kalarakis, V.N. Burganos, and A.C. Payatakes, Phys. Rev. E **65**, 056702 (2002).
[15] A.N. Kalarakis, V.N. Burganos, and A.C. Payatakes, Phys. Rev. E **67**, 016702 (2003).
[16] Y.H. Qian, D. D'Humieres, and P. Lallemand, Europhys. Lett. **17**, 479 (1992).
[17] X. Shan and H. Chen, Phys. Rev. E **49**, 2941 (1994).
[18] K. Langaas and J.M. Yeomans, Eur. Phys. J. B **15**, 133 (2000).
[19] L.D. Landau and E.M. Lifshitz, *Fluid Mechanics*, 2nd ed. (Pergamon press, 1987).